*Health Physics* Vol. 57, Sup. 1, pp. 21–27, 1989
Printed in the U.S.A.

0017-9078/89 $3.00 + .00


## ● *Biological Factors in Modeling: Respiratory Tract*

# FLOW DISTRIBUTION IN HUMAN AND CANINE TRACHEOBRONCHIAL AIRWAY CASTS

B. S. Cohen and J. K. Briant
Institute of Environmental Medicine, New York University Medical Center, New York, NY 10016

*Abstract*—**Measurements of flow rates through hollow casts of human and canine tracheobronchial airways, which extend from just below the larynx to airways 1 mm in diameter, show basic similarities in the distribution of air flow and also species differences which must be considered. The distribution of air flow, for both constant and pulsatile inspiratory flow, was measured for minute volumes equivalent to 6, 11, 17 and 22 L min$^{-1}$ for the human and 3, 6, 8, and 11 L min$^{-1}$ for the dog. Inertia of air flow (inertance) was found to carry more of the flow to airways of the lower lobes at higher flow rates. Basic differences in airway branching pattern result in a more distinct change in airflow distribution as flow rate changes for the canine cast as compared with the human cast. These differences should contribute to differing patterns of mass transfer of inhaled particles and gases in central airways of the two species.**

## INTRODUCTION

THE DEPOSITION pattern of inhaled particles on the epithelial surfaces of tracheobronchial airways can be an important determinant of the dose to critical respiratory tract tissues. To establish reliable dose-response relationships, and to extrapolate results from animal inhalation studies to humans, it is essential to know the deposition patterns and efficiencies within airways in both human and animal species. Both the deposition of airborne particles, and the mass transfer of gases and vapors, may be expected to differ in the lungs of experimental animals from those in humans because basic differences in their airway branching patterns will result in different airflow patterns. Lippmann and Schlesinger (1984) have considered how species differences might affect intrabronchial deposition. They suggest that important distinctions result not only from the differences in size, but also from the differences in the anatomy and branching pattern of lung airways. These include variations in the fraction of total lung deposition which occurs in the tracheobronchial tree, and the pattern of deposition, which is expected to vary because of the assumed differences in airway branching patterns and airflow profiles.

Distribution of air flow in the lungs is influenced by the dynamic and complex interaction of many factors. Jackson et al. (1987) present a model which includes six parametric factors: resistance and inertance, both in the airways and in parenchymal tissue, compliance of lung tissue, and compliance of the gas itself. When the distribution of air flow is measured in essentially rigid, hollow airway casts, only airway resistance and inertia of the air flow are variable factors. Differences in the geometries of canine and human airways result in different inertance which will, in part, determine the flow distributions. The way in which inertance will change with flow rate may differ in the two species. The work reported here compares the measured flow distribution in full hollow airway casts of the human and canine tracheobronchial trees. The morphometry of these models is reported, and the dimensions of the human model are compared with the Weibel Model A (Weibel 1963).

Past use of hollow airway casts of the human tracheobronchial tree has provided detailed quantitative information on intrabronchial particle deposition which cannot be obtained from *in vivo* tests, nor from idealized tubular models (Schlesinger and Lippmann 1972; Schlesinger et al. 1977; Gurman et al. 1984; Cohen 1986). Chan et al. (1980) detailed the airflow artifacts seen in simple, smooth-walled model systems as compared with those in tracheobronchial casts. Their results are evidence that measurements in morphometrically realistic models are needed for realistic studies of deposition. The casts used for our work, prepared from whole lungs obtained at autopsy, have been developed for the study of air flow and mixing characteristics, and the effect of flow patterns on the deposition of gases and particles. This work provides new quantitative data on airflow distribution in a realistic central airway cast for two species and for two different airflow patterns: steady inspiratory flow and pulsatile inspiratory flow.

## EXPERIMENTAL METHODS

### *Cast preparation and morphometry*

Two hollow airway casts were produced: one human and one canine (Fig. 1). The human lung was obtained from a 45-y-old male (wt: 59 kg, ht: 1.7 m). The canine

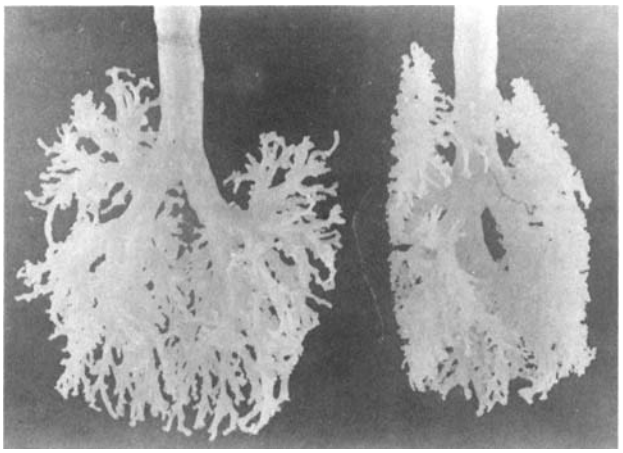

Fig. 1. Hollow Si rubber casts of human (left) and canine (right) central airways. Terminal airways are <1 mm in diameter.

lung was from a mixed-breed animal (approximate wt: 22 kg). The whole lungs were freeze-dried while inflated to a pressure of 2.5 kPa (25 cm $H_2O$), which was believed to correspond to full vital capacity of the lungs. Chevalier et al. (1978) demonstrated that the shape of an *in vivo* lung was identical to the excised lung inflated with no transpulmonary gradient at full vital capacity. Total lung volumes after fixing were 5.2 L and 2.2 L for the human and dog lungs, respectively. Individual lobar volumes were not measured to avoid disrupting lung structure. The airways were cast with microcrystalline petroleum wax (Schlesinger et al. 1977) to the level of the terminal bronchioles. In order to completely cast all regions to this level in the canine lung, it was necessary to permit the wax to penetrate more deeply in some regions. The lung tissue was macerated from the cast, using concentrated NaOH. The solid cast was then pruned back to retain airways larger than about 0.5 mm.

Each airway was identified using the binary nomenclature illustrated in Fig. 2. Morphometric measurements included airway branch midpoint diameter, length, and branching angle as defined by Raabe et al. (1976). The branching, or flow, angle is the angle between the centerline of the airway and that of the parent airway. Measurements were made on the wax casts through the fifth generation for all branches, and to the terminal airways along three single paths of our models: a major branch path which follows the larger airway at each bifurcation; a minor branch path, selecting the smaller branch at each bifurcation; and a path which alternately selects major and minor branches. All branches secondary to the three primary paths were also measured.

Hollow casts were produced by coating the solid wax casts with silicone rubber.* Many thin layers were necessary in order to preserve the distinction of the small terminal airways. Thicker layers were added to the larger airways for mechanical support. Each terminal airway was trimmed open, and the wax was melted out of the positive cast. Residual wax was removed by washing the cast in hot oil. There were more than 1000 terminal airways in each hollow cast.

*Airflow measurement*

During the experiments, the human (or canine) hollow cast was attached to a calibrated pneumotachograph (Fleisch number 1) to monitor the supply of air into the trachea. The distribution of air flow was measured at constant flow rates of 15, 30, 45, and 60 L $min^{-1}$ for the human cast, and 7.5, 15, 22.5, and 30 L $min^{-1}$ for the canine. These are equivalent to minute volumes of 6, 11, 17, and 22 L $min^{-1}$, respectively, for the human and 3, 6, 8, and 11 L $min^{-1}$ for the canine casts, assuming a breathing pattern of $\frac{3}{8}$ inspiration, $\frac{3}{8}$ expiration with pauses of $\frac{1}{8}$ of a cycle after inspiration and expiration. Flow-rate values used for the canine model were chosen to be one-half those used in the human model because the dog lung was nearly half the size of the human. These values are consistent with a minute volume of 2.9 L $min^{-1}$, reported for anesthetized dogs of about the same size as that from which our cast was made (Altman and Dittmer 1971). Tracheal Reynolds numbers (Re) ranged from 1140 to 4560 in the human cast and 520 to 2090 in the dog cast. Fourth-generation Re ranged from about 240 to 980 and 100 to 400 for the human and dog, respectively.

The pressure drop through the cast was less than 10 Pa (1 mm $H_2O$), which made it difficult to make a measurement without perturbing the flow distribution. Therefore, a pressure balancing system was devised (Fig. 3). The segment of the cast peripheral to the branch to be measured was sealed into a plastic bag, connected via a flow balance valve to a soap-film flow meter. The entire cast was sealed into the outer chamber, which connected to a separate exhaust flow restriction valve. A horizontal tube containing a soap film was placed between the outer

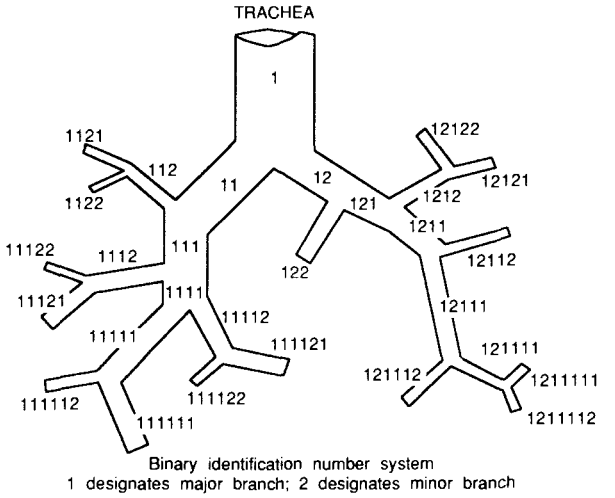


Fig. 2. Airway segment labels uniquely identify each segment according to branching pattern; 1 denotes major and 2 denotes minor branches (Raabe et al. 1976).

* Dow Corning 3145 RTV, Dow Corning Corp., Midland, MI 48640.

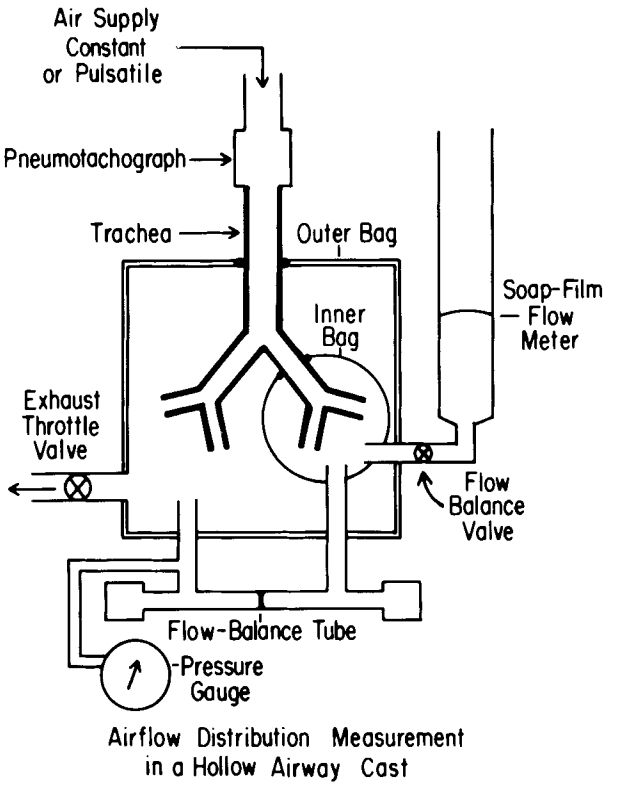


Fig. 3. Schematic diagram of flow distribution measurement system. Flow balance circuit was used to maintain equal pressure in inner and outer bags with a stationary soap film.

chamber and the inner bag containing the segment. The pressure balance between the sections was maintained by adjusting the exhaust and flow-balance valves.

The values of flow distribution measured with this apparatus for steady flow are remarkably precise and reproducible. The pressure balance was more difficult to control for pulsatile flow, but an average balance was maintained over the course of a pulse. Test measurements showed that the sum of flows measured in the individual airways was within 3% of the tracheal flow in all cases under these conditions. This demonstrates that the average pressure balance is a reasonable method for measurement of pulsatile flow distribution.

Pulsatile flow was obtained by using a positive-pressure respirator,[†] with a switching valve[‡] to simulate inspiratory flow cycles. The flow was monitored by electronically integrating[§] the pneumotachograph signal. The pulse rate was 30 $min^{-1}$ with a 1-s inspiratory pulse followed by a 1-s pause. Mean inspiratory flow rate was determined from the measured integrated flow volume and pulse duration. The flow pulses were nearly square in shape; thus, the peak flow velocity was only about 25% greater than the mean. Measurements of the flow distribution under pulsatile flow were compared with that for constant inspiratory flow for equivalent mean inspiratory flow rates in the trachea.

The basic model system did not include a larynx. A separate set of measurements was carried out for the human lung cast, with a model larynx added to the system to test for any effect this may have had on the flow distribution.

*Analytical methods*

The measured flow rates in a given airway segment for different flow rates into the trachea were fitted by linear regression to an equation of the form $y = ax^b$, where $y$ = the flow rate in the airway segment, $x$ = the tracheal flow rate, and $a$ and $b$ are fitted parameters. When $b$ is near unity, $a$ represents the fraction of the total flow which passes through the segment. The coefficient of determination ($r^2$) was calculated for each regression of four (or more) different flow rates.

## RESULTS

The number of airway generations from the trachea (generation 0) to the terminal airway of the cast for each of the three complete pathways is shown in Table 1. Also shown is the diameter of the smallest airway. The airway branching pattern along the major pathway is very similar for the human and canine casts, with the paths terminating on the dorsal edge of the caudal side of the lower right lobe. Differences in branching pattern are more apparent in the upper lobes; however, the minor and alternating pathways terminate near one another on both the human and canine casts: on the dorsal side, near the junction of the upper left and lower left lobes. Table 2 presents a summary of the morphometric data for the human cast through the tenth generation. Table 3 presents the same data for the canine cast. All airways were measured through the fifth generation; beyond that, only selected pathways are represented.

Flow distribution is represented by the calculated values $a$ and $b$ of the power curves, which are shown in Table 4 for one complete set of airways for each cast. The coefficient of determination ($r^2$) is also given for each airway. Airways listed in Table 4 are representative of the many which were measured. Although not exactly the same set of airways was measured on each cast, many corresponding airway segments were measured. Values of $b$ greater than one show that, as airflow increases in the

Table 1. Number of airway generations per path through the human and canine airway models (diameter of smallest airway, mm).

| | Minor | Alternate | Major |
|---|---|---|---|
| Human | 8 (0.7) | 10 (0.8) | 29 (0.4) |
| Canine | 7 (0.5) | 8 (0.5) | 28 (0.6) |

[†] Monaghan 170C, J. J. Monaghan Co., 500 Alcott St., Denver, CO 80204.

[‡] Rudolph 1400, Hans Rudolph Co., 7200 Wyandotte St., Kansas City, MO 64114.

[§] Validyne FV156, Validyne Engineering Corp., P.O. Box 9025, Northridge, CA 91328.

Table 2. Morphometry of the human cast for the first 10 generations. Length and diameter for the Weibel Model A (Weibel 1963) are shown for comparison. All airways are included for generations 0 to 5 (see text).

| Generation | Number of Airways | Length (mm) | Diameter (mm) | Flow Angle (degrees) | Weibel Model A | |
|---|---|---|---|---|---|---|
| | | | | | Length (mm) | Diameter (mm) |
| 0 | 1 | 100.0 | 18.6 | 0 | 120 | 18.0 |
| 1 | 2 | 43.3 (0.43)[a] | 13.2 (0.11) | 38.5 (0.13) | 47.6 | 12.2 |
| 2 | 4 | 15.9 (0.44) | 8.6 (0.16) | 38.8 (0.68) | 19.0 | 8.3 |
| 3 | 8 | 11.6 (0.63) | 6.6 (0.13) | 38.2 (0.67) | 7.6 | 5.6 |
| 4 | 16 | 12.1 (0.38) | 5.4 (0.22) | 34.6 (0.87) | 12.7 | 4.5 |
| 5 | 32 | 11.0 (0.47) | 4.9 (0.26) | 31.6 (0.81) | 10.7 | 3.5 |
| 6 | 6 | 11.3 (0.20) | 3.5 (0.44) | 22.2 (0.95) | 9.0 | 2.8 |
| 7 | 6 | 8.0 (0.38) | 3.1 (0.72) | 39.5 (0.76) | 7.6 | 2.3 |
| 8 | 6 | 8.8 (0.90) | 2.5 (0.80) | 28.7 (1.0) | 6.4 | 1.9 |
| 9 | 4 | 5.2 (0.68) | 2.8 (0.51) | 32.0 (1.3) | 5.4 | 1.5 |

[a]Mean (coefficient of variation)

trachea, a larger fraction of the flow goes to the airway segment. Values less than one mean that a smaller fraction of the flow goes to the segment with increasing tracheal flow rate. For $b = 1$, the fraction flowing through the airway does not change as flow rate into the trachea changes. Measured flow values can be combined for appropriate bifurcating networks to obtain parameters for particular lung segments, single lobes, or for each lung. For a complete pair of lungs, the value of $b$ is 0.991 for the canine and 1.006 for the human during steady inspiration. The precision of the measurements was estimated from replicate experiments. There was generally much less than 1% difference between replicates. Maximum variability was 5%.

Airways listed in Table 4 are separated into upper (cranial) and lower (caudal) lung segments. The value of $b$ is less than one for most airways in the upper lobes and greater than one for airways in lower lobes. For both canine and human casts, this is most apparent for the upper left and lower right lobes, indicating a redistribution of flow from the upper to the lower lobes as the flow rate increases. The difference is more striking in the canine lung, where the pattern is more consistent. The pattern is similar for pulsatile flow, which also further increases the deviation from linearity for a given airway. For $b$ values less than one, a binomial sign test finds that $b$ is consistently lower for pulsatile flow than for steady flow ($p < 0.05$) in both canine and human casts.

Table 3. Morphometry of the canine cast for the first 10 generations. All airways are included for generations 0 to 5 (see text).

| Generation | Number of Airways | Length (mm) | Diameter (mm) | Flow Angle (degrees) |
|---|---|---|---|---|
| 0 | 1 | 227.5 | 20.3 | 0 |
| 1 | 2 | 20.6 (0.10)[a] | 18.4 (0.11) | 26.0 (0.49) |
| 2 | 4 | 15.3 (0.37) | 11.8 (0.36) | 30.0 (1.3) |
| 3 | 8 | 9.5 (0.62) | 9.1 (0.44) | 38.8 (0.75) |
| 4 | 16 | 9.7 (0.50) | 6.6 (0.47) | 23.1 (0.95) |
| 5 | 32 | 6.0 (0.47) | 4.6 (0.58) | 30.2 (1.1) |
| 6 | 6 | 6.1 (1.1) | 4.1 (0.94) | 43.3 (0.66) |
| 7 | 6 | 1.3 (1.3) | 4.0 (1.2) | 18.0 (2.2) |
| 8 | 6 | 8.2 (0.93) | 5.5 (0.84) | 27.5 (0.13) |
| 9 | 2 | 3.1 (1.4) | 7.4 (0.30) | 15.0 (1.4) |

[a]Mean (coefficient of variation)

The coefficient of variation of $b$ for all air flows measured in each cast increased from 0.21 for steady flow to 0.24 for pulsatile flow in the canine cast, and from 0.13 to 0.16 in the human cast. This is comparable to the coefficient of variation of 0.09 found by Slutsky et al. (1980) for nearly the same number of airways with steady flow through a human cast. The cast used in that work differed from ours in that it terminated with airways of 3 to 4 mm in diameter. This suggests that the presence of the smaller airways in our cast affected the flow distribution in the larger airways.

In all cases, when measured flows for the upper and lower lobes of the right or left lung are added, the value of $b$ for the lung is closer to one than it is for individual lobes (Table 4). Some difference in the value of $b$ remains between the left and right lungs: It is slightly greater for the right lung than for the left, for the canine cast, with both steady and pulsatile inspiration. This pattern is similar for the human cast with steady inspiration, but of lesser magnitude. These differences between left and right whole lungs are small compared to differences between individual airways of upper and lower lobes for both species. The distribution of lobar flow rates for human and dog casts are compared in Fig. 4. They could not be compared with lobar volume because the volumes were unknown. On an ordinate basis, lobar flow rate corresponds to lobar volume.

The presence of a model larynx was found to have little influence on airflow distribution in the human cast. All measurements on a complete set of distribution pathways showed less than 5% difference from steady inspiratory flow measured without the larynx. For most mea-

Table 4. Flow distributions for both steady inspiratory (a) and pulsatile (b) flow are listed as parameters of a linear regression to the equation $y = ax^b$.

| (a) | | Canine | | | Human | | |
|---|---|---|---|---|---|---|---|
| Airway | | *a* | *b* | $r^2$ | *a* | *b* | $r^2$ |
| Upper | | | | | | | |
| Left | 12222 | 0.0072 | 0.928 | 0.988 | 0.0392 | 0.710 | 1.000 |
| | 1222 | 0.0683 | 0.726 | 0.999 | 0.1171 | 0.899 | 1.000 |
| | 12212 | 0.0398 | 0.664 | 0.993 | 0.0371 | 1.101 | 0.999 |
| | 12211 | 0.1060 | 0.706 | 0.992 | 0.0468 | 1.058 | 1.000 |
| | 1212 | 0.0334 | 0.863 | 0.996 | 0.1077 | 0.805 | 0.999 |
| Right | 1122 | 0.0529 | 0.810 | 0.997 | 0.0666 | 0.980 | 1.000 |
| | 1121 | 0.1758 | 0.766 | 0.998 | 0.1294 | 1.019 | 1.000 |
| Lower | | | | | | | |
| Left | 12112 | 0.0650 | 1.132 | 0.998 | 0.0472 | 1.062 | 0.999 |
| | 12111 | 0.1589 | 1.066 | 0.999 | 0.1237 | 1.062 | 1.000 |
| Right | 1112 | 0.0641 | 1.094 | 0.999 | 0.0715 | 1.059 | 1.000 |
| | 11112 | 0.0495 | 1.184 | 0.999 | 0.0783 | 0.899 | 0.999 |
| | 111112 | 0.0405 | 0.962 | 1.000 | 0.0598 | 0.925 | 1.000 |
| | 1111112 | 0.0542 | 1.147 | 0.999 | 0.0493 | 0.960 | 0.999 |
| | 111111 | 0.2808 | 1.035 | 0.995 | 0.1558 | 1.014 | 0.999 |
| | 1111111 | 0.2285 | 0.998 | 0.993 | 0.0906 | 1.083 | 1.000 |
| Left Lung | | 0.4344 | 0.974 | 1.000 | 0.4591 | 1.002 | 1.000 |
| Right Lung | | 0.6338 | 1.002 | 0.999 | 0.5365 | 1.009 | 1.000 |
| Total Lungs | | 1.0680 | 0.991 | 1.000 | 0.9955 | 1.006 | 1.000 |

| (b) | | Canine | | | Human | | |
|---|---|---|---|---|---|---|---|
| Airway | | *a* | *b* | $r^2$ | *a* | *b* | $r^2$ |
| Upper | | | | | | | |
| Left | 12222 | 0.0131 | 0.696 | 0.933 | | | |
| | 1222 | 0.0833 | 0.647 | 0.996 | 0.1222 | 0.860 | 1.000 |
| | 12212 | 0.0470 | 0.588 | 0.994 | 0.0392 | 1.059 | 0.999 |
| | 12211 | 0.1310 | 0.612 | 1.000 | 0.0397 | 1.073 | 1.000 |
| | 1212 | 0.0434 | 0.744 | 0.993 | 0.1179 | 0.758 | 0.999 |
| Right | 1122 | 0.0544 | 0.766 | 0.995 | 0.0706 | 0.945 | 1.000 |
| | 1121 | 0.2221 | 0.656 | 0.995 | 0.1323 | 0.989 | 1.000 |
| Lower | | | | | | | |
| Left | 12112 | 0.0626 | 1.116 | 0.998 | 0.0360 | 1.103 | 0.998 |
| | 12111 | 0.1741 | 1.005 | 0.999 | 0.1337 | 1.018 | 0.999 |
| Right | 1112 | 0.0598 | 1.087 | 1.000 | 0.0790 | 1.007 | 1.000 |
| | 11112 | 0.0473 | 1.167 | 0.999 | 0.0914 | 0.836 | 0.998 |
| | 111112 | 0.0461 | 0.885 | 0.997 | 0.0571 | 0.920 | 1.000 |
| | 1111112 | 0.0510 | 1.132 | 0.997 | 0.0507 | 0.932 | 0.999 |
| | 111111 | 0.2323 | 1.072 | 0.999 | | | |
| | 1111111 | 0.1821 | 1.051 | 0.999 | 0.0898 | 1.062 | 1.000 |
| Left Lung | | 0.4717 | 0.919 | 1.000 | 0.4521 | 0.978 | 1.000 |
| Right Lung | | 0.5925 | 0.995 | 1.000 | 0.5570 | 0.976 | 1.000 |
| Total Lungs | | 1.0596 | 0.965 | 1.000 | 1.0090 | 0.977 | 1.000 |

surements the difference was less than 1%. Since the canine larynx is farther removed from the bronchial carina than is the human larynx, there would be even less difference for the canine lung.

## DISCUSSION

The redistribution of flow with increased flow rate recorded here has also been reported by others for both canine (Snyder and Jaeger 1983) and human (Slutsky et al. 1980; Sussman et al. 1985) central airway casts. Those casts included airways 3 mm in diameter and larger; our casts include all airways 1 mm diameter and larger, and along many paths they extend to airways 0.5 mm in diameter.

The significant redistribution of flow to the lower lung that was seen here for increasing steady flows was a result of the increased inertia of the air mass which is distributed through bifurcations. Haselton and Scherer (1980) discussed the effect of the shape of the bronchial

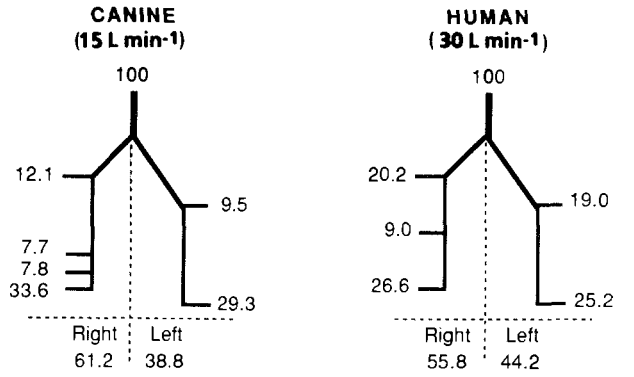


Fig. 4. Lobar flow-rate distributions for corresponding flows through human and canine airway casts. Values shown are for steady inspiratory flow.

bifurcation on flow profiles. They showed that the shape is important for mixing of gases and particles between inspired and functional residual air. This shape is also related to the inertial quality of flow through the bifurcations.

Olson et al. (1973) have shown that flow profiles in the central airways are complex, partly because of the geometry of the airways and the asymmetric branching pattern. Also, at typical inspiratory flow rates (a few to 120 L $min^{-1}$), the Reynolds numbers are such that flow changes from turbulent to laminar and back, and turbulence produced in upper airways can be carried distally on inspiration through several branching levels before being dissipated by viscous forces. The changing flow profiles result in altered mass transfer between the air and the surface area of the airway lining, which allows hot spots of deposition of gas or aerosol particles. More air passes close to these relatively hot spots than to other regions of the airway surface, which should result in enhanced mass transfer. Olson et al. (1970) have suggested that the most important factor in determining flow profiles in the bronchi is the effect of entrance length, which is the distance needed to establish the parabolic velocity profile normally associated with laminar flow. They predict that for a tracheal flow rate of 10 L $min^{-1}$, the entrance length will be greater than the tube length down to the 10th branching level (bronchioles) in the human tracheobronchial tree. For 20 L $min^{-1}$, the entrance length will be greater than the total length of the airway to the 13th branching level. The flow profile developed at each branch point will change with flow rate and may contribute to the change in distribution seen in these casts.

Pulsatile inspiratory flow, in our model system, is more realistic than steady flow. The inertial effects seen for constant flow appear to be enhanced by pulsatile flow. For pulsatile flow the $b$ values are consistently lower in the canine upper lobes than for constant flow, as can be seen in Table 4. Differences are not so apparent in the pulsatile flow measurements in the human cast. This difference between the species is reasonable when the path of air flow is considered with respect to the value of $b$. It appears that if there are more sharp bends along the path, then the flow is impeded, as shown by a reduced value of $b$. This effect is especially apparent in the canine upper lobes, where the airway branching pattern is most different from that of the human airways. Conversely, fewer bends along the path minimizes impedance, which should allow relatively more air flow, shown by a $b$ value greater than one. This is especially noticeable in the lower lobes.

It may be assumed that downstream conditions must be considered when examining inertial effects on flow distribution. Other investigators have made measurements at the open ends of central airways, omitting the influence of more peripheral airways. The casts used in our study extend to airways well beyond those airway segments in which flow was measured; any influence of the immediate downstream flow field is thus included.

The distributions of air flow in the canine and human central airways are very similar, but the work reported here shows that the differences must be considered when studying deposition in these airways. This is particularly evident from the more dramatic way in which the flow distribution changes with flow rate for canine than for human morphometry. *In vivo*, the inertial effect on distribution of air flow is probably damped by lung tissue compliance, and the tendency of air flow to redistribute from the upper to the lower lobes at higher flow rates may be less pronounced. Nonetheless, studies of deposition in these hollow casts of human and canine tracheobronchial airways, especially at lower flow rates, should provide realistic comparisons of mass transfer to airway surfaces.

*Acknowledgments*—This work was supported by Special Emphasis Research Career Award Grant No. 00022 from the National Institute for Occupational Safety and Health of the Centers for Disease Control and Grant No. ER60592 from the Department of Energy. It is part of a center program supported by Grant ES 00260 from National Institute of Environmental Health Sciences and Grant CA13343 from the National Cancer Institute. The authors thank Dr. I. Nathan, who provided the canine lungs; R. Blumenthal and J. Brandes, who helped with the morphometric measurements; and A. Vendetti, who assisted with entering data in computer files.

## REFERENCES

Altman, P. L.; Dittmer, D. S. Respiration and circulation, biological handbook. Bethesda, MD: Federation of American Societies for Experimental Biology; 1971.

Chan, T. L.; Schreck, R. M.; Lippmann, M. Effect of the laryngeal jet on particle deposition in the human trachea and upper bronchial airways. J. Aerosol Sci. 11:447–459; 1980.

Chevalier, P. A.; Rodarte, J. R.; Harris, L. D. Regional lung expansion at total lung capacity in intact vs. excised canine lungs. J. Appl. Physiol. 45:363–369; 1978.

Cohen, B. S. Deposition of ultrafine particles in the human tracheobronchial tree. In: Hopke, P. K., ed. Radon and its decay products. Washington, DC: American Chemical Society; 1986:475–486.

Gurman, J. L.; Lioy, P. J.; Lippmann, M.; Schlesinger, R. B.

Particle deposition in replicate casts of the human upper tracheobronchial tree under constant and cyclic inspiratory flow: I. Experimental. Aerosol Sci. Technol. 3:245–252; 1984.
Haselton, F. R.; Scherer, P. W. Bronchial bifurcations and respiratory mass transport. Science 208:69–71; 1980.
Jackson, A. C.; Lutchen, K. R.; Dorkin, H. L. Inverse modeling of dog airway and respiratory system impedances. J. Appl. Physiol. 62:2273–2282; 1987.
Lippmann, M.; Schlesinger, R. B. Interspecies comparisons of particle deposition and mucociliary clearance in tracheobronchial airways. Toxicol. Environ. Health 13:441–469; 1984.
Olson, D. E.; Dart, G. A.; Filley, G. F. Pressure drop and fluid flow regime of air inspired into the human lung. J. Appl. Physiol. 28:482–494; 1970.
Olson, D. E.; Sudlow, M. F.; Horsfield, K.; Filley, G. F. Convective patterns of flow during inspiration. Arch. Intern. Med. 131:51–57; 1973.
Raabe, O. G.; Yeh, H. C.; Schum, G. M.; Phalen, R. F. Tracheobronchial geometry: Human, dog, rat, hamster, LF-53. Springfield, VA: NTIS; 1976.
Schlesinger, R. B.; Lippmann, M. Particle deposition in casts of the human upper tracheobronchial tree. Am. Ind. Hyg. Assoc. J. 33:237–251; 1972.
Schlesinger, R. B.; Bohning, D. E.; Chan, T. L.; Lippmann, M. Particle deposition in a hollow cast of the human tracheobronchial tree. J. Aerosol Sci. 8:429–445; 1977.
Slutsky, A. S.; Berdine, G. G.; Drazen, J. M. Steady flow in a model of human central airways. J. Appl. Physiol. 49:417–423; 1980.
Snyder, B.; Jaeger, M. J. Lobar flow patterns in a hollow cast of canine central airways. J. Appl. Physiol. 54:749–756; 1983.
Sussman, R. G.; Cohen, B. S.; Lippmann, M. The distribution of airflow in casts of human lungs. In: Proceedings of the American Association for Aerosol Research. Albuquerque, NM: American Association for Aerosol Research; 1985:226.
Weibel, E. R. Morphometry of the human lung. Berlin: Springer-Verlag; 1963.

## QUESTIONS AND COMMENTS

(Paper presented by J. K. Briant, Institute of Environmental Medicine, New York University Medical Center, New York, NY.)

**Q:** J. F. Park, Pacific Northwest Laboratory, Richland, WA

What were the sizes of the dog and human used in making the lung casts?

**Briant:** The two-dimensional photograph of the airway casts is not a good indication of relative size in terms of volume. Canine lungs are long and narrow relative to human lungs. Even though the canine lungs of this study had cranial-caudal length comparable to human lungs, they were less than half the volume. Measurement of the total volume of each specimen was made by volume displacement in water for the sealed, freeze-dried lungs; human: 5.2 L; canine: 2.2 L.